REPORT DOCUMENTATION PAGE

Form Approved
OMB No. 0704-0188

1. REPORT DATE *(DD-MM-YYYY)*	2. REPORT TYPE	3. DATES COVERED *(From - To)*
02-28-2012	Final Performance Report	May 2009 – Nov. 2011

4. TITLE AND SUBTITLE

Low Noise Interband Cascade Photodetectors

5a. CONTRACT NUMBER
FA9550-09-1-0288

5b. GRANT NUMBER

5c. PROGRAM ELEMENT NUMBER
AFOSR

6. AUTHOR(S)
Rui Q. Yang

5d. PROJECT NUMBER
090248

5e. TASK NUMBER

5f. WORK UNIT NUMBER

7. PERFORMING ORGANIZATION NAME(S) AND ADDRESS(ES)

University of Oklahoma
110 West Boyd Street
Norman, OK 73019

8. PERFORMING ORGANIZATION REPORT NUMBER

AFOSR-004FPR

9. SPONSORING / MONITORING AGENCY NAME(S) AND ADDRESS(ES)

Air Force Office of Scientific Research
Dr. Kitt Reinhardt
875 N. Randolph Street
Arlington, VA 22203

10. SPONSOR/MONITOR'S ACRONYM(S)
AFOSR

11. SPONSOR/MONITOR'S REPORT NUMBER(S)
AFRL-OSR-VA-TR-2013-0064

12. DISTRIBUTION / AVAILABILITY STATEMENT

Distribution is unlimited

13. SUPPLEMENTARY NOTES

14. ABSTRACT

This report documents the investigations and development of low noise interband-cascade infrared photodetectors (ICIPs) at the University of Oklahoma (in collaborations with others) for a period of time from May 2009 to Nov. 2011. ICIPs, composed of discrete superlattice (SL) absorbers, are demonstrated at temperatures up to 350K in the mid-infrared spectral region. The peak responsivity exceeds 200 mA/W, suggesting a significantly enhanced quantum efficiency of the SL absorbers. We showed that ICIP device performance such as background-limited performance (BLIP) temperature can be modified and thus improved by the design of the intraband relaxation zone with quantum engineering. The efficient extraction of photo-excited carriers in ICIPs was also demonstrated by our study of photo-response spectra on the dependence of bias voltage. We have recently demonstrated ICIPs with the Johnson-noise limited detectivity (D^*) exceeding 10^{12}, 10^{11}, 10^{10}, 10^9 Jones at 80, 160, 230, 300 K, respectively. It is expected that optimized ICIPs will provide improved performance by combining the advantages of conventional photodiodes and the discrete nature of QWIPs and interband cascade lasers.

15. SUBJECT TERMS
Semiconductor infrared photodetectors, quantum wells, type-II superlattices, interband cascade structures.

16. SECURITY CLASSIFICATION OF: Unclassified			17. LIMITATION OF ABSTRACT	18. NUMBER OF PAGES	19a. NAME OF RESPONSIBLE PERSON
a. REPORT	b. ABSTRACT	c. THIS PAGE			19b. TELEPHONE NUMBER *(include area code)*
			UU	8	Rui Q Yang 405-325-7361

Final Performance Report
For a period from May 2009 to Feb. 2012 on
An AFOSR Project (Award Number: FA9550-09-1-0288)

Low Noise Interband Cascade Photodetectors

Rui Q. Yang
School of Electrical and Computer Engineering, University of Oklahoma, Norman, OK 73019

February 28, 2012

Program Manager: Dr. Kitt Reinhardt
Air Force Office of Scientific Research
875 N. Randolph Street, Arlington, VA 22203

Abstract

This report documents the investigations and development of low noise interband-cascade infrared photodetectors (ICIPs) at the University of Oklahoma (in collaborations with others) for a period of time from May 2009 to Nov. 2011. ICIPs, composed of discrete superlattice (SL) absorbers, are demonstrated at temperatures up to 350K in the mid-infrared spectral region. The peak responsivity exceeds 200 mA/W, suggesting a significantly enhanced quantum efficiency of the SL absorbers. We showed that ICIP device performance such as background-limited performance (BLIP) temperature can be modified and thus improved by the design of the intraband relaxation zone with quantum engineering. The efficient extraction of photo-excited carriers in ICIPs was also demonstrated by our study of photo-response spectra on the dependence of bias voltage. We have recently demonstrated ICIPs with the Johnson-noise limited detectivity (D^*) exceeding 10^{12}, 10^{11}, 10^{10}, 10^9 Jones at 80, 160, 230, 300 K, respectively. It is expected that optimized ICIPs will provide improved performance by combining the advantages of conventional photodiodes and the discrete nature of QWIPs and interband cascade lasers.

I. Introduction

This is the first final performance report from the University of Oklahoma (OU) for project entitled "Low noise interband cascade photodetectors". The performance period of this project is from May 2009 to Nov. 2011.

Our objective is to develop a new class of low noise mid-infrared (3-5 μm) detectors--interband cascade (IC) infrared photodetectors (ICIPs) based on type-II quantum-well (QW) and superlattice (SL) heterostructures. The project includes device design, MBE growth, device fabrication and characterization. Significant progress has been made and was reported in technical conferences (two invited) and three journal articles [1-7]. Below, some details are provided.

II. Detailed Device Performance of ICIPs

II.A. Operation Principle

The operation principle of the proposed ICIP is illustrated in Fig. 1. Similar to an IC-laser structure, an ICIP structure is composed of multiple stages connected in series that take advantage of the broken-gap alignment in type-II QW structures for facilitating carrier transport. However, unlike an IC laser, where a forward bias is required for device operation, an ICIP can be operated at zero bias. As shown in Fig. 1, each stage is divided into three zones based on three different processes: (1) excitation, (2) intraband relaxation, and (3) interband tunneling. Figure 1 shows a section of an ICIP structure including three excitation zones (absorbers) connected with the intraband relaxation (2) and interband tunneling zones (3). These zones also act as a hole barrier (2) and an electron barrier (3), respectively, forming a complementary barrier configuration similar to that in Ref. [8]. To understand the operation of this structure as a detector, we describe the role of each zone associated with a photo-excited electron moving through the structure. In zone (1), photons excite electrons from state E_h in the valence band to state E_e in the conduction band. The electrons then move to the left through intraband relaxation in zone (2), while holes are confined in zones (1) and (3). The transport of electrons to the right is greatly suppressed because state E_e is located within the bandgap of zone (3) based on the GaSb/AlSb QWs. Zone (2) is constructed with digitally-graded multiple InAs/AlSb QWs to form an energy ladder with discrete energy levels (*e.g.* E_1, E_2, …). That is, the right end of the energy ladder is near the conduction band of the adjoining absorber, while the left end of the profile is near the valence band of the absorber adjoining it. After zone (2), electrons return to the valence band state in the adjacent absorber through interband tunneling facilitated by the type-II band-edge alignment in zone (3). Based on this IC structure, a photocurrent is achieved even without an external bias voltage because of the overall asymmetric band profile of this structure.

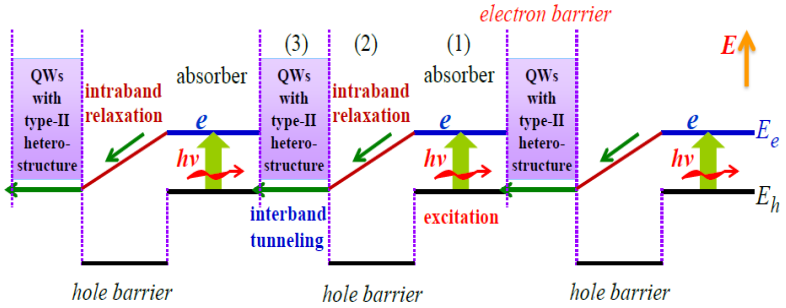

Fig. 1. Illustration of operation principle of IC photodetector.

In contrast to other types of photodetectors, there are several distinct features for ICIPs that are noteworthy. **1.** The photo-excited electrons in the active region are transferred to the bottom

of the energy ladder with a nearly 100% escape probability. This high probability is because the intersubband relaxation time (~1 ps) is much shorter than the interband recombination time (~1 ns in a typical situation or ~0.1 ns at higher temperatures with increased Auger recombination). **2.** The interband tunneling time in the type-II heterostructure is on the order of picoseconds or shorter with a thin barrier. This tunneling mechanism enables the quick and efficient removal of holes after photo-excitation. The combined effect of efficient collection of both photo-excited electrons and holes translates to high quantum efficiency for one cascade stage with a relatively thick (< the electron diffusion length) absorber (*e.g.* a superlattice (SL) excitation zone as shown in Fig. 2, instead of a single period of type-II QWs), resulting in enhanced absorption, and higher responsivity compared to typical QWIPs. And **3.** In contrast to detectors based on intersubband transitions, where normal incidence absorption is prohibited by quantum-mechanical selection rules, ICIPs are inherently sensitive to normal-incidence radiation. In summary, ICIPs promise to provide high performance in terms of efficient carrier transport and sensitivity to normal incidence radiation.

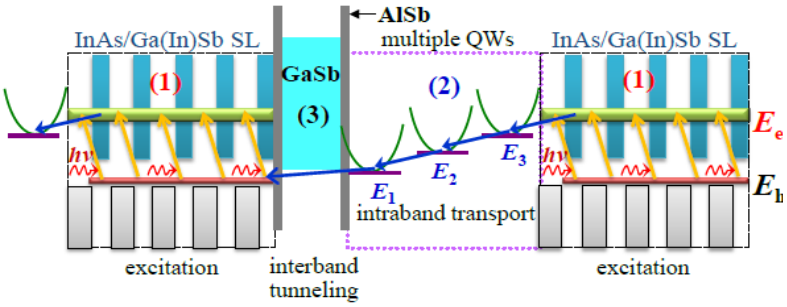

II.B. Initial Demonstration

Two ICIPs have been designed and grown with finite SL absorbers with cut-off wavelength near 5 μm at 80 K. The ICIP structure, grown by MBE, has 7 identical cascade stages, and each stage has a ~0.15-μm-thick SL absorber that is composed of 28 periods of InAs/GaSb (9 ML/9 ML). The two ICIP wafers (denoted as EB2700 and EB2807) have the same absorbers with different intraband relaxation zones for investigating transport effects on device performance.

The devices made from the ICIP wafers operated at temperatures up to 350K with a cutoff wavelength near 5 μm at 80 K to beyond 7 μm above room temperature. As shown in Fig. 3 for a deep etched 60-μm-diameter device (denoted EB2702-7D-G) from wafer EB2702, the peak responsivity exceeds 200 mA/W, much higher than the values (*e.g.* 35 mA/W) reported for quantum cascade (QC) detectors and (*e.g.* 46 mA/W) obtained from early IC laser structures operated as detectors. This demonstrates significantly enhanced quantum efficiency with the use of the finite SL absorbers.

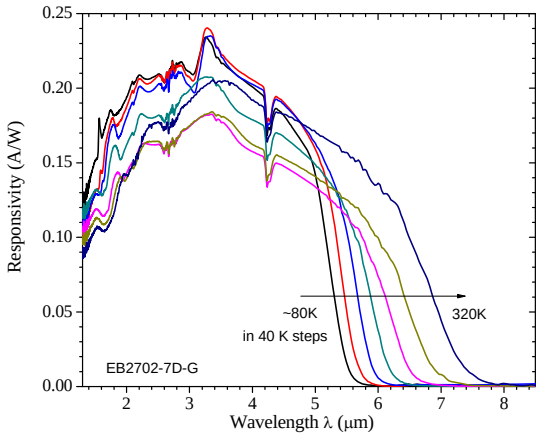

Fig. 3. Responsivity spectra of EB2702-7D-G at different temperatures.

The efficient extraction of photo-excited carriers in ICIPs was also demonstrated by our study of photo-response spectra on the dependence of bias voltage as shown in Fig. 4. As one can see, the carrier extraction is already

efficient at zero bias and the measured response spectra are relatively insensitive (variation <15%) to the bias voltage.

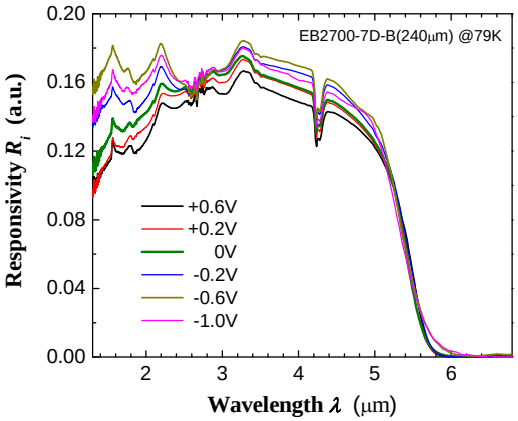

Fig. 4. Response spectra of an ICIP device at various bias voltages.

From the current-voltage characteristics, we can extract the product of the device resistance R_0 and the area A, which is shown in Fig. 5 for three devices at 0 and -20 mV. R_0A at low temperatures in Fig. 5 is underestimated due to the RT background radiation resulting from the absence of a cold shield in our measurement apparatus, particularly for the shallow-etched device EB2702-2S-D where lateral diffusion and collection of photogenerated carriers is expected to be substantial. From Fig. 5, one can see that R_0A exhibited different temperature dependences for devices made from wafers EB2700 and EB2702. This suggests that we can manipulate device transport properties by adjusting the design of the intraband relaxation zone.

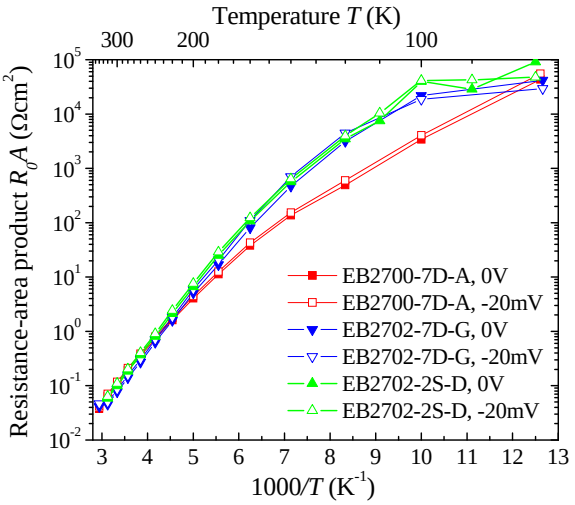

Fig. 5. R_0A for three devices at 0 V and -20 mV.

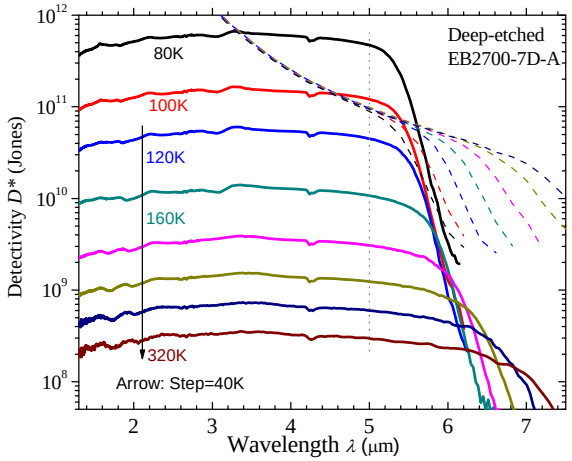

Fig. 6. Johnson noise limited (solid) and background limited (dashed) D^* for device EB2700-7D-A at -20 mV.

From the responsivity spectra and measured R_0A, one can estimate the Johnson-noise limited and background limited detectivity (D^*). Fig. 6 shows D^* for device EB2700-7D-A at various temperatures at a bias of -20 mV. At low temperatures, the Johnson-noise limited D^* approaches 10^{12} Jones and the device is background limited. At room temperature, the Johnson-noise limited D^* is about 4.2×10^8 Jones at 5 μm, which is comparable to state-of-art type-II SL detectors and nBn SL detectors. The achievable Johnson-noise limited D^* is actually higher than what is shown in Fig. 6, since R_0 increases with biases more negative than -20 mV at high temperatures. For example, the Johnson-noise-limited D^* values at a wavelength of 5 μm and 300 K are 6.0×10^8 and 1.1×10^9 at -0.2 V and -0.6 V, respectively. However, the dark-current increases with increasingly negative bias and the device performance eventually becomes dark-current-shot-noise-limited. This occurs at a bias more negative than -0.2 V for EB2700-7D-A at 300 K. In

Fig. 7, D^* at a wavelength of 5 μm is plotted for two deeply-etched devices at -20 mV and 0V. From Fig. 7, one can find that the background-limited performance (BLIP) temperatures (below which the noise is dominated by the background photons) are ~126 K and 105 K for devices made from wafers EB2702 and EB2700, respectively, at a wavelength of 5 μm. Again, the results demonstrated that device performance such as BLIP temperature can be modified and thus improved by the design of the intraband relaxation zone with quantum engineering. The total internal quantum efficiency (QE) at 5 μm is about 26% even though the total thickness of absorbers is less than 1.5 μm, which is significantly higher than the value from typical QWIPs with a similar number of absorbers.

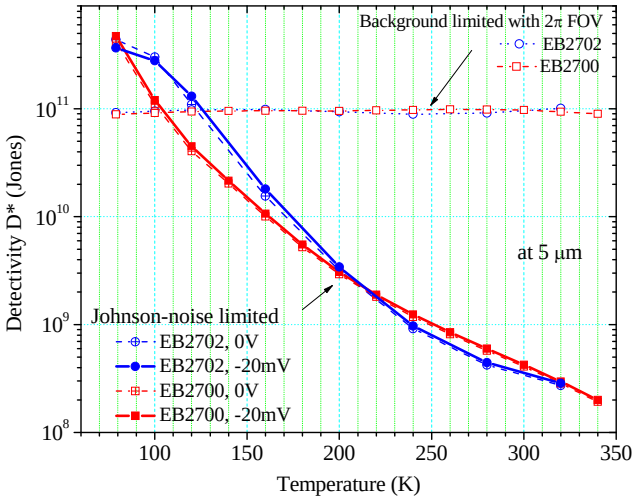

Fig. 7. Johnson noise limited and background limited D^* at 5 μm wavelength for two devices at 0 V and -20 mV.

We also did studies on material growth and used one IC laser structure to have observed a clear photon current response with a cutoff wavelength beyond 7 μm at 80 K, even though the structure was not designed for use as a detector.

II.C. Recent Results

The ICIP wafers studied recently consist of a 7-stage interband cascade structure using a finite InAs/GaSb type-II SL as an absorber. Three different discrete SL absorber designs were investigated: the absorber in sample A is comprised of 30-period InAs/GaSb SL (0.15 μm) with Be-doping concentration of 1×10^{17} cm^{-3}, sample B1 has the same absorber thickness but a higher Be-doping (3×10^{17} cm^{-3}), and sample B2 has the sample Be-doping (1×10^{17} cm^{-3}) but a thicker absorber (50-period of InAs/GaSb SL, 0.25-μm-thick). The samples were grown on (001) GaSb substrates in a molecular beam epitaxy (MBE) system equipped with group-III SUMO cells and group-V crackers. The electron barrier consists of AlSb/GaSb/AlSb/GaSb/AlSb QWs with layer sequential thickness of 16/53/16/75/21 (Å) to suppress the direct tunneling through the electron barrier, which is enhanced compared to our earlier ICIPs [1]. The intraband tunneling time across this double GaSb/AlSb QW is estimated to be longer than 100 μs based on a two-band $k\cdot p$ model. Such an intraband tunneling time is orders of magnitude longer than other time scales such as interband tunneling time through the type-II broken gap and carrier recombination lifetime, and thus effectively shuts off the intraband tunneling channel if the defect states in the gap could be ignored. Also note that this suppression of the intraband tunneling current is achieved without blocking the interband tunneling channel.

These ICIP wafers were processed into deep-etched photodetectors with mesas ranging from 110 to 400 μm in diameter, by using standard contact UV lithography followed by tartaric-acid based wet-chemical etching. Electrical performance of these ICIPs is characterized for different temperatures ranging from 80 K up to 340 K. The dark current densities at -50 mV are as low as 2.1 nA/cm^2 at 80 K, and 2.7 μA/cm^2 at 150 K, which is over two orders of magnitude lower than

what was observed in the previous ICIPs [1], indicating excellent suppression of dark current by the enhanced electron barrier. Experimental evidence of this suppression is provided by the abrupt increase of current at a large reverse bias (-4.5 V), which was observed in all three devices. This rectification breakdown is shown in Fig. 8 for sample B. The abrupt increase in the reverse current is most likely due to a breakdown of the electron barrier at large reverse bias, so that the electron barrier no longer effectively blocks the inter-stage tunneling and the device becomes photoconductive. The breakdown of the current rectification at large reverse bias (-4.5 V) could be an indication of near resonance of the electron miniband in the SL absorber with the electronic state of the conduction band in the double GaSb/AlSb QW, resulting in the breakdown of the electron barrier. Also, clear sawtooth features with seven negative differential resistance regions are observed, which are manifested more clearly by extracted differential conductance curve in the inset of Fig. 8. Such features are indicative of good material quality and quantum transport associated with energy level alignments. With the suppression of dark current, we demonstrated ICIPs with the Johnson-noise limited detectivity (D^*) exceeding 10^{12}, 10^{11}, 10^{10}, 10^{9} Jones at 80, 160, 230, 300 K, respectively (Fig. 9), which is comparable to state-of-the-art type-II SL detectors [9] and nBn SL detectors [10]. More details are reported in Ref. 3.

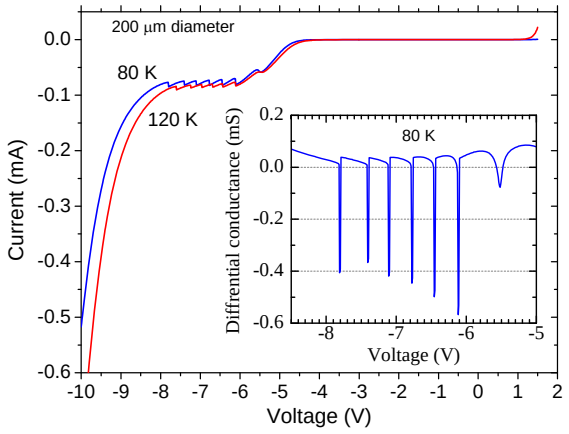

Fig. 8. *I-V* characteristics of an ICIP. The inset is the differential conductance of the device at 80 K.

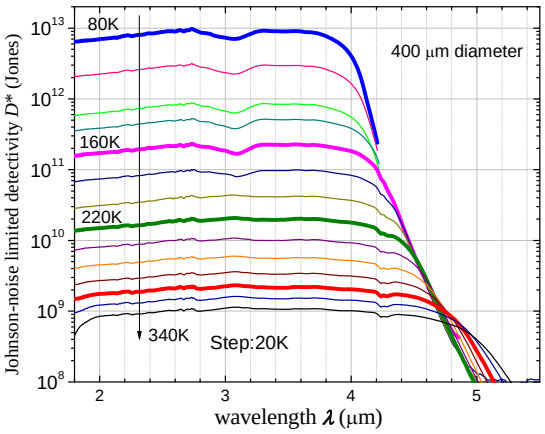

Fig. 9. Johnson noise limited D^* for an ICIP device.

III. Further Remarks

The characteristics of ICIPs that have investigated and demonstrated in this project have suggested a great potential of these devices to achieve high performance needed for many applications. The flexibility of ICIP architecture coupled with quantum engineering should provide considerable improvements in several aspects of device performance, which merits further development. These results from our preliminary studies are encouraging. Nevertheless, because ICIPs are new and relatively complicated, with many interfaces and strained thin layers, their growth by MBE is challenging. Thus, ICIP devices are still in their infancy and aspects of the underlying physics are not yet well understood. Extensive research toward improving the material quality and deepening our understanding of their operation is therefore needed to fulfill their promise for practical applications. Furthermore, extension to other aspects is promising based on unique features of ICIPs. For example, in contrast to the continuous absorber design in a conventional photodiode, ICIPs employ a discrete absorber architecture (similar to QWIPs)

where electrons move quickly across a short distance in an individual absorber and are capable of *high-speed* operation without compromising absorption quantum efficiency, while still suppressing noise and maintaining reasonably-high detectivity. These high-speed ICIPs will be desirable particularly with the use of lasers for applications such as free-space communication and heterodyne detection. With the development and availability of high-performance room temperature QC and IC lasers in the mid- to long-wave IR spectrum, one can expect the growing demands and applications of high-speed detectors that are capable of operating at TE cooler temperatures with high performance. Currently, only limited QWIPs that typically operated in cryogenic temperatures are available in high-speed operation.

IV. Proof of Concept Demonstration of a New Type of Energy Conversion Device

A photovoltaic (PV) device based on an interband cascade (IC) structure is proposed for efficiently converting solar and thermal energy to electricity. These IC PV devices employ absorption and transport regions with characteristics that are favorable for achieving high open-circuit voltage and thus possibly improving conversion efficiency over conventional PV devices. Preliminary experiments carried out using ICIP (7 stages) and IC laser (11 stages) structures showed open-circuit voltages that exceed the single-bandgap voltage from these devices under infrared illumination. The observed open-circuit voltage demonstrates multiple stages operating in series and provides an initial proof of concept for IC PV devices. The details are already published in Applied Physics Letters [2].

Acknowledgements

The work was carried out in collaboration with John F. Klem at Sandia National Laboratories, Zhaobing Tian, Zhihua Cai, R. T. Hinkey, L. Li, Tetsuya D. Mishima, Michael B. Santos, and Matthew B. Johnson at the University of Oklahoma (OU), D. Lubyshev, Y. Qiu, J. M. Fastenau, and W. K. Liu at IQE Inc., H. C. Liu at National Research Council, Canada. Gratitude is also to Edward Aifer of NRL for useful discussions. Research at OU was supported in part by a new faculty start-up fund at OU, by NSF (award No. 0838439) for initial study, by AFOSR (award No. FA9550-09-1-0288), and by C-SPIN, the Oklahoma/Arkansas MRSEC (DMR-0520550).

References

1. R. Q. Yang, Z. Tian, Z. Cai, J. F. Klem, M. B. Johnson, and H. C. Liu, "Interband cascade infrared photodetectors with superlattice absorbers", J. Appl. Phys. **107**, No. 5, 054514 (2010).
2. R. Q. Yang, Z. Tian, J. F. Klem, T. D. Mishima, M. B. Santos, and M. B. Johnson, "Interband cascade photovoltaic devices", Appl. Phys. Lett. **96**, No. 6, 063504 (2010).
3. Z. Tian, R. T. Hinkey, R. Q. Yang, D. Lubyshev, Y. Qiu, J. M. Fastenau, W. K. Liu, M. B. Johnson, "Interband Cascade Infrared Photodetectors with enhanced electron barriers and *p*-type superlattice absorbers", J. Appl. Phys. **111**, 024510 (2012).
4. Z. Tian, Z. Cai, R. Q. Yang, T. D. Mishima, M. B. Santos, M. B. Johnson, and J. F. Klem, "Interband Cascade Infrared Photodetectors", Quantum Sensing and Nanophotonic Devices VII, Photonics West, San Francisco, CA, January 23-28, 2010, CA, USA (in Proc. SPIE 7608, paper 76081X).

5. R. Q. Yang, Z. Tian, Z. Cai, J. F. Klem, T. D. Mishima, M. B. Santos, M. B. Johnson, "Quantum-Engineered Interband Cascade Infrared Photodetectors" (**invited**), at 10th International Conference on Mid-Infrared Optoelectronics Materials and Devices, Shanghai, China, Sept. 5-9, 2010.
6. Z. Tian, R. Q. Yang, D. Lubyshev, Y. Qiu, J. M. Fastenau, W. K. Liu, J. F. Klem, M. B. Johnson, "Development of Interband Cascade Infrared Photodetectors", Infrared Technology and Applications XXXVII (SPIE Conference 8012), April 25-29, 2011, Orlando, FL, USA. (in Proc. SPIE 7587, paper 80122U).
7. R. Q. Yang, "Interband Cascade Infrared Photodetectors" (**invited**), Quantum Sensing and Nanophotonic Devices IX, Photonics West, San Francisco, CA, January 22-26, 2012, CA, USA.
8. D. Z.-Y. Ting, C. J. Hill, A. Soibel, S. A. Keo, J. M. Mumolo, J. Nguyen, and S. D. Gunapala, "A high-performance long wavelength superlattice complementary barrier infrared detector," *Appl. Phys. Lett*. **95**, 023508 (2009).
9. Y. Wei, A. Hood, H. Yau, A. Gin, M. Razeghi, M. Z. Tidrow, and V. Nathan, "Uncooled operation of type-II InAs/GaSb superlattice photodiodes in the midwavelength infrared range", Appl. Phys. Lett. **86**, 233106 (2005).
10. J. B. Rodriguez, E. Plis, G. Bishop, Y. D. Sharma, H. Kim, L. R. Dawson, and S. Krishna, "*nBn* structure based on InAs/GaSb type-II strained layer superlattices", Appl. Phys. Lett. **91**, 043514 (2007).